BIOCHEMISTRY
including biophysical chemistry & molecular biology

Article

pubs.acs.org/biochemistry

Mg^{2+}-Linked Self-Assembly of FtsZ in the Presence of GTP or a GTP Analogue Involves the Concerted Formation of a Narrow Size Distribution of Oligomeric Species

Begoña Monterroso,[†] Rubén Ahijado-Guzmán,[†] Belén Reija,[‡] Carlos Alfonso,[†] Silvia Zorrilla,[‡] Allen P. Minton,[§] and Germán Rivas*[,†]

[†]Centro de Investigaciones Biológicas, and [‡]Instituto de Química-Física "Rocasolano", Consejo Superior de Investigaciones Científicas, Madrid, Spain

[§]Section on Physical Biochemistry, Laboratory of Biochemistry and Genetics, National Institute of Diabetes and Digestive and Kidney Diseases, National Institutes of Health, Bethesda, Maryland 20892, United States

Supporting Information

ABSTRACT: The assembly of the bacterial cell division FtsZ protein in the presence of constantly replenished GTP was studied as a function of Mg^{2+} concentration (at neutral pH and 0.5 M potassium) under steady-state conditions by sedimentation velocity, concentration-gradient light scattering, fluorescence correlation spectroscopy, and dynamic light scattering. Sedimentation velocity measurements confirmed previous results indicating cooperative appearance of a narrow size distribution of finite oligomers with increasing protein concentration. The concentration dependence of light scattering and diffusion coefficients independently verified the cooperative appearance of a narrow distribution of high molecular weight oligomers, and in addition provided a measurement of the average size of these species, which corresponds to 100 ± 20 FtsZ protomers at millimolar Mg^{2+} concentration. Parallel experiments on solutions containing guanosine-5′-[(α,β)-methyleno]triphosphate, sodium salt (GMPCPP), a slowly hydrolyzable analogue of GTP, in place of GTP, likewise indicated the concerted formation of a narrow size distribution of fibrillar oligomers with a larger average mass (corresponding to 160 ± 20 FtsZ monomers). The closely similar behavior of FtsZ in the presence of both GTP and GMPCPP suggests that the observations reflect equilibrium rather than nonequilibrium steady-state properties of both solutions and exhibit parallel manifestations of a common association scheme.

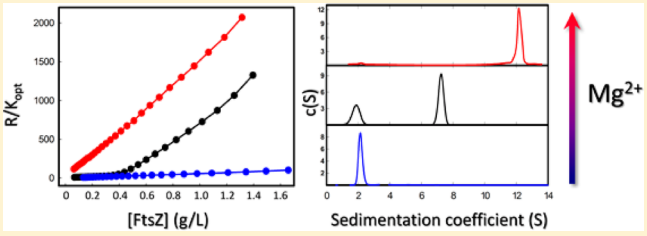

FtsZ is an essential protein required for septation in most bacteria, in archaea, and in some organelles. It is an early septum component, it forms a ring at midcell, and it is thought to be responsible for initiating and driving cell constriction.[1−4] FtsZ shares homology with eukaryotic tubulin, as well as its GTPase activity and its capacity to polymerize. The self-association of FtsZ in the presence of GDP and its polymerization in the presence of GTP have been studied extensively.[4,5] While the mechanism of GDP-FtsZ oligomer formation is relatively well understood, that is not the case for the GTP-linked FtsZ polymerization. In the presence of GTP, FtsZ polymerizes in an apparently cooperative manner to form single stranded protofilaments that, depending upon solution and working conditions (buffer composition, temperature, protein density, surface effects, excluded volume and electrostatic nonspecific effects of macromolecular additives, specific effects of other cell division proteins) can adopt a variety of supramolecular structures: flexible single and multistranded fibers, circles, ribbons, bundles, and toroids.[1,2,4,6−8] This polymorphism is due to the structural plasticity of FtsZ polymers: it would take only a very small free energy perturbation to change the structural organization of the intermolecular interface and bring about large changes in the geometry of the fibers.[9]

Erickson and co-workers have established that FtsZ polymers are highly dynamic both in vivo[10] and in vitro.[11] In the former study, they bleached part of a fluorescent Z-ring in a bacterium that has been engineered to produce fluorescent FtsZ and observed that the fluorescence recovers in ca. 10−30 s.[10] While this finding establishes a dynamic exchange of FtsZ between the Z-ring and the cytoplasm, the implications for the kinetics or pseudoequilibria governing fiber or Z-ring assembly are not at all clear. The dynamic character of FtsZ polymers linked to the GTPase activity of the protein constitutes an additional challenge to study FtsZ assembly in the presence of GTP, which requires special procedures for the maintenance of polymer stability throughout the duration of a typical biochemical and biophysical experiment.[6] The variety of quantitative techniques that have been applied to study FtsZ assembly is consequently low compared to the variety of

Received: February 29, 2012
Revised: May 8, 2012
Published: May 8, 2012

techniques utilized to study other protein assembly systems. Moreover, different research groups have studied assembly under differing solution conditions (pH, ionic strength, buffer composition). These facts may in part explain disagreements that have arisen during the last few years regarding the mechanism of FtsZ polymerization in the presence of GTP.[2,9]

The dependence on protein concentration of the sedimentation coefficient distribution of FtsZ in the presence of GTP and Mg^{2+} was measured by sedimentation velocity.[9] In that study, an enzymatic GTP regenerating system (RS) was added to the solutions to avoid GTP depletion, and hence polymer disassembly, during sufficient time to perform the sedimentation velocity measurements reported under steady-state conditions. The data clearly showed a system consisting of a well separated slowly sedimenting fraction and a rapid species. With increasing total protein concentration, the abundance of the slowly sedimenting fraction was reduced while the amount of the fast species increased. The rapid fraction corresponded to a finitely sized distribution of species with an *s*-value of around 13 S, which did not grow indefinitely upon increasing protein concentration. This behavior resembled a condensation reaction in which the condensed species was soluble and with a relatively narrow size distribution.

The motivation of this work is to confirm and extend the previous experimental observations, to obtain a model-free estimate of the oligomer size and the dependence of oligomer size upon Mg^{2+} concentration, to verify the existence of a phase transition-like cooperativity of oligomer formation on the assembly pathway, and to test whether this concerted transition reflects or not a quasi-equilibrium behavior and does not derive from a precarious balance of competing hydrolytic and nucleotide exchange reactions far from equilibrium. With these goals, we have carried out parallel studies of FtsZ assembly using a combination of biophysical methodologies (sedimentation velocity, concentration gradient static and dynamic light scattering, and fluorescence correlation spectroscopy) to more clearly elucidate the nature of the self-assembly process under a well-defined set of experimental conditions, close to physiological (neutral pH, 0.5 M potassium). These studies were done over a broad range of Mg^{2+} and protein concentrations under working conditions comparable to those utilized in previous work.[9] Experiments were first performed with FtsZ under steady-state conditions in the presence of GTP and the GTP-RS. To assess the possible contribution of effects arising from GTP hydrolysis and nucleotide exchange on the behavior of the system, parallel experiments were conducted in the presence of GMPCPP, a GTP analogue that is hydrolyzed at a rate that is only 2% that of FtsZ-catalyzed hydrolysis of GTP under the conditions of our experiments.[12]

EXPERIMENTAL PROCEDURES

Materials. Guanine nucleotides were from Jena. Other analytical grade chemicals were from Sigma. Even if not specifically mentioned, in all the GTP-induced assembly experiments the GTP was regenerated using a GTP-regenerating system (1 unit/mL acetate kinase, 15 mM acetyl phosphate) as previously described[6] to maintain the stability of FtsZ polymers at steady-state during the time scale of the experiments. When the assembly was triggered with GMPCPP, the stability of the polymers was even greater than in the case of GTP + RS, as measured by time-dependent light scattering.

FtsZ Purification and Labeling. *Escherichia coli* FtsZ was purified by the Ca^{2+}-induced precipitation method as described[5] and stored at −80 °C in the ionic exchange elution buffer. Immediately before use, FtsZ was dialyzed in the working buffer (50 mM Tris-HCl, pH 7.5, 500 mM KCl) supplemented with the specified concentrations of $MgCl_2$ or EDTA. Protein labeling with Alexa 488 carboxylic acid succinimidyl ester dye was performed in polymeric form as described in detail elsewhere,[13,14] rendering labeled FtsZ that behaves as the unlabeled protein in terms of polymerization.[6,14] The Alexa 488 dye was selected for being highly photostable, very bright, and quite hydrophilic. The degree of labeling of FtsZ, estimated from the molar absorption coefficients of the fluorophore and the protein, was 30−50%.

Sedimentation Velocity (SV). The experiments were carried out in a Beckman Optima XL-I ultracentrifuge (Beckman-Coulter) equipped with interference optics that allows monitoring FtsZ sedimentation at physiological (mM) GTP concentrations. FtsZ (0.5−1 g/L) was equilibrated in working buffer (over a broad range of Mg^{2+} concentrations) and, just before the sedimentation experiment, supplemented with millimolar GTP or GMPCPP. FtsZ samples were centrifuged at 30 000 rpm and 25 °C using an An50Ti eight-hole rotor and double-sector Epon-charcoal centerpieces. The elapsed time between the addition of GTP + RS (or GMPCPP) and the last scan used in the analysis of the data was less than 60 min, an interval of time short enough to ensure a constant concentration of GTP and maintenance of polymer stability throughout. Differential sedimentation coefficient distributions $c(s)$ were calculated by least-squares boundary modeling of the experimental data using SEDFIT.[15]

Static Light Scattering (CG-SLS). *Multiangle Light Scattering.* Measurements of angular dependence of scattering over a broad range of FtsZ concentrations were carried out in a DAWN-EOS multiangle light scattering photometer equipped with a Calypso system (Wyatt Technology Corp, Santa Barbara) consisting of a software-controlled multiple syringe pump used to create the concentration gradient and an Optilab rEX differential refractometer configured to collect data in parallel from the incoming sample stream. All components of the GTP-RS were supplemented at each gradient step to maintain constant concentration of these components throughout the FtsZ gradient. Data were collected at 20 °C with 1% sensitivity of the detectors. The raw data acquired consist of the time-dependent scattering intensity at 14 scattering angles and the time-dependent differential refractive index. The Rayleigh ratio was calculated from the raw scattering intensity, and the w/v concentration of protein, *w*, calculated from the differential refractive index as described in refs 16 and 17, except that an empirical constant of proportionality between *dRI* and *w* was used to calculate the w/v concentration as a function of time. The results are expressed as the concentration and angle-dependent Rayleigh ratio $R(w,\theta)$ in units of an optical constant

$$K_{opt} = \frac{4\pi^2 n_0^2}{N_A \lambda_0^4}\left(\frac{dn}{dw}\right)^2 \quad (1)$$

where n_0, N_A, and λ_0 denote the solvent refractive index, Avogadro's number and the vacuum wavelength of incident light (690 nm), respectively, and dn/dw is the specific refractive index increment of the protein, taken as 0.185 cm^3/g.[17]

90° Scattering. Measurements of the dependence of scattering intensity at 90° upon FtsZ concentration were performed in a modified mini-DAWN light scattering photometer (Wyatt Technology Corp., Santa Barbara) using an

dx.doi.org/10.1021/bi300401b | *Biochemistry* 2012, 51, 4541−4550

automated dilution protocol as described.[18] The composition of the sample solution and the dilution buffer was the same to maintain constant concentration of all the components present in the GTP and GMPCPP solutions throughout the process of FtsZ dilution. Preliminary measurements of scattering intensity established that FtsZ species formed in the presence of GTP plus RS or GMPCPP were stable over periods of time far exceeding the duration of a dilution experiment. Concentration of protein at each dilution step was calculated from the initial concentration, and raw scattering intensity data were converted to the scaled Rayleigh ratio $R(w,90°)/K_{opt}$ as described in ref 18.

Dynamic Light Scattering Assays (DLS). DLS experiments were carried out in a Protein Solutions DynaPro MS/X instrument (Protein Solutions, Piscataway, NJ) at 25 °C using a 90° light scattering cuvette. Previous to measurements, samples were filtered twice with 0.1 μm Anotop 10 Plus filters (Whatman) and subsequently centrifuged during 30 min at 100000*g* and 4 °C. Data were collected and exported as text files with Dynamics V6 Software, and analyzed using user-written scripts and functions in MATLAB (Ver. 7.10, MathWorks, Natick, MA). Data correspond to a minimum of two independent measurements each of which was the average of at least seven replicates.

DLS data are reported in the form of an autocorrelation function describing the time-dependence of the correlation between scattering intensity at any given time and the intensity at a subsequent increment of time τ. For a single scattering species, the autocorrelation function is given by[19]

$$\mathrm{ACF}(\tau) = \mathrm{ACF}_\infty + (\mathrm{ACF}_0 - \mathrm{ACF}_\infty)\exp(-2Dq^2\tau) \quad (2)$$

where

$$q = \frac{4\pi n_0}{\lambda_0}\sin\left(\frac{\pi}{4}\right)$$

ACF_0 and ACF_∞ respectively denote the values of ACF in the short and long time limits, q denotes the scattering vector at 90°, n_0, and λ_0 are the solvent refractive index and the wavelength of incident light, and D is the translational diffusion coefficient of the scattering species. In the present work, the scattering arises from an as-yet-undefined mixture of scattering species, and in this case the autocorrelation function is more appropriately described by an empirical exponential function of the kind used for analysis of the slowly sedimenting component of fibrinogen fibrin and protofibrils.[20]

$$\mathrm{ACF} = \mathrm{ACF}_\infty + (\mathrm{ACF}_0 - \mathrm{ACF}_\infty)\exp[-(D_{app}q^2\tau)^\beta]^2 \quad (3)$$

where D_{app} represents an apparent average diffusion coefficient, and β is a parameter that decreases from unity with the width of the distribution of diffusion coefficients. For each set of experimental conditions, eq 3 was fit to experimental autocorrelation functions via nonlinear least-squares to obtain the best-fit value of the apparent diffusion coefficient, which was then corrected to a standard temperature and solvent viscosity (20 °C, water) for comparison with the results obtained by other techniques. Since D_{app} is an average, it may vary with total protein concentration when the protein is undergoing equilibrium self-association.

Fluorescence Correlation Spectroscopy Assays (FCS). FCS measurements were carried out under two-photon excitation on a MicroTime 200 system (PicoQuant, Berlin, Germany) with the setup described elsewhere.[14] 5−10 autocorrelation curves were acquired for each sample during 1 min each at 21 °C and globally analyzed with the FFS Data Processor software (Scientific Software Technologies Center, Belarus)[21] using the following expression, in which it is assumed that the samples are excited by a three-dimensional Gaussian beam:

$$G(\tau) = 1 + G(0)\sum_i [f_i(1 + \tau/\tau_{Di})^{-1}(1 + \tau/S^2\tau_{Di})^{-1/2}] \quad (4)$$

where $G(0)$ is the amplitude of the autocorrelation function. S is a structure parameter ($S = z_0/r_0$ where r_0 and z_0 are the lateral and axial dimensions of the effective detection volume), which varied from 3 to 6 as determined by calibration with fluorescein or rhodamine 110 solutions. τ_{Di} is the translational diffusion time of the fluorescent particle i ($\tau_{Di} = r_0^2/8D_i$, for two-photon excitation, where D_i is the translational diffusion coefficient). The r_0 value was estimated from the calibration assuming D of 4×10^{-6} cm^2/s and 4.4×10^{-6} cm^2/s for fluorescein and rhodamine 110, respectively.[22−24] f_i is the fractional contribution of species i to the autocorrelation function. A two species model was fit to the autocorrelation curves for samples containing unpolymerized FtsZ-Alexa 488,[14] the faster one indicating the presence of minor fractions (∼10−20%) of free dye in the samples and the other one corresponding to the unassembled protein. The fast component was also found in the solutions containing assembled FtsZ, and its translational diffusion time was fixed to that measured for Alexa 488 in the same buffer (corresponding to a $D \sim 4 \times 10^{-6}$ cm^2/s). Preparations of labeled protein containing different amounts of free dye rendered translational diffusion coefficients equivalent within the error for the polymer. To fit the autocorrelation traces obtained in the presence of GTP or GMPCPP, two other components corresponding to the slowly diffusing polymeric species and to unassembled protein were required.[14] The translational diffusion time of the unpolymerized protein was fixed to that obtained for FtsZ in the absence of GTP or GMPCPP (corresponding to a $D \sim 5 \times 10^{-7}$ cm^2/s), and its contribution varied depending on the total FtsZ concentration in the solution and on the buffer conditions. Slight variations in the fraction of unassembled FtsZ (for a given buffer and protein concentration) were observed depending on the preparation of labeled protein used, which, however, did not have any effect on the translational diffusion coefficient retrieved for the polymeric species. D values given here were normalized to standard conditions (20 °C, water) and represent the average of at least three independent measurements.

The concentration of FtsZ-Alexa 488 was typically 0.006 g/L (150 nM), and the final protein concentration was achieved by adding unlabeled protein. No significant changes in the spectral properties of the Alexa 488 dye were observed upon incorporation of the protein to the polymers,[14] and equivalent autocorrelation curves were obtained at different distances (from 10 to 30 μm) from the coverslip surface. Some measurements of the translational diffusion coefficient of assembled FtsZ were also performed using fluorescein or tetramethylrhodamine labeled FtsZ with the same result as reported here for the Alexa 488 labeled protein.

Estimate of Molar Mass of FtsZ Polymers from Hydrodynamic Measurements. The apparent molar mass of a single sedimenting solute species, M, may be calculated

dx.doi.org/10.1021/bi300401b | *Biochemistry* 2012, 51, 4541−4550

using measured values of the sedimentation coefficient s and the diffusion coefficient D according to the Svedberg equation[25]

$$M = \frac{RT}{(1 - \bar{\nu}\rho)} \frac{S_{20,w}}{D_{20,w}} \quad (5)$$

where T, R, and ρ respectively denote the absolute temperature, the universal gas constant, and the density of the solution and $\bar{\nu}$ the partial specific volume of the solute. It is stressed that since the frictional coefficients for sedimentation and diffusion cancel in the derivation of eq 5, the estimate of molar mass obtained via this relation is valid independent of the structure of the sedimenting/diffusing species. As described in the Results, at high magnesium concentration both sedimentation and diffusion measurements indicate the presence of a narrow size distribution of oligomeric species. We assume that the Svedberg relation holds approximately for such a distribution[26] and utilize the average value of s obtained from analysis of sedimentation velocity and the average of the D values obtained from analysis of dynamic light scattering and fluorescence correlation spectroscopy.

RESULTS

Sedimentation Velocity. Distributions of sedimentation coefficients, obtained from SEDFIT analysis of the sedimenting boundaries, are plotted in Figure 1 for 1 g/L FtsZ solutions prepared at different Mg^{2+} concentrations in the presence of millimolar GTP supplemented with the GTP-regenerating system. At millimolar magnesium, >95% of the protein sedimented with an experimental s-value of around 13 S, while the corresponding GDP-form of FtsZ sedimented as a mixture of monomers and dimers, with s-values around 3 and 4 S, confirming our previous observations.[9] The sedimentation coefficient distribution of GTP-FtsZ polymers changed dramatically upon lowering the Mg^{2+} concentration. At cation concentrations between 10 and 100 μM, the sedimentation data were well described by two main sedimenting species with s-values around 2.5 and 6−7 S, respectively. The relative concentration of these two species changed with Mg^{2+} (the 2.5 S species predominating at lower Mg^{2+}), a characteristic feature of Mg^{2+}-linked self-association reactions.[5] In the presence of EDTA, the protein sedimented as a single peak with s-value of 2.5 S, compatible with a protein monomer whose shape deviates from the expected behavior of a globular protein.

The sedimentation velocity data obtained at a protein concentration of 0.5 g/L in the presence of GMPCPP at various magnesium concentrations (Figure 2) qualitatively resemble those obtained with GTP, indicating a highly concerted formation of FtsZ polymers. At millimolar Mg^{2+},

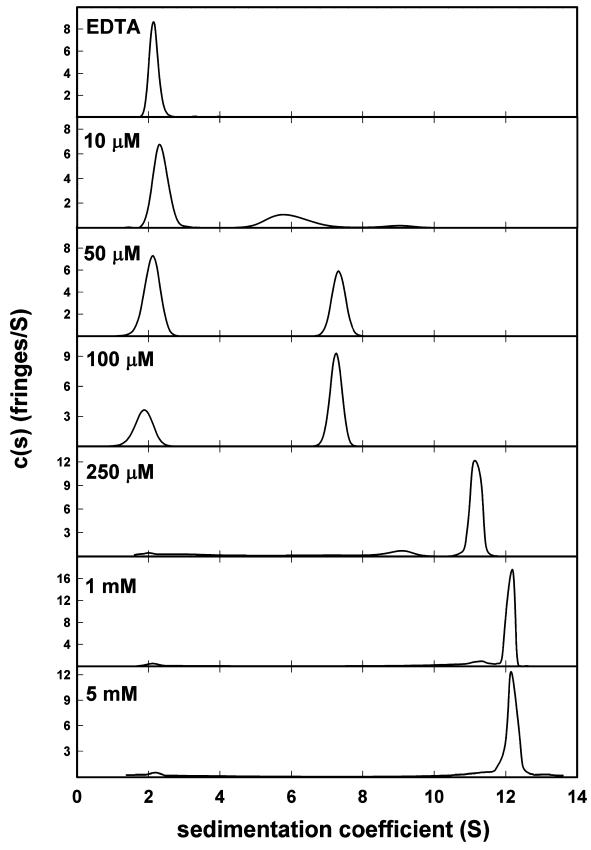

Figure 1. Mg^{2+} dependence of FtsZ sedimentation velocity in the presence of 1 mM GTP + GTP-RS: Sedimentation profiles of 1 g/L FtsZ equilibrated in working buffer at the magnesium concentrations specified in the figure.

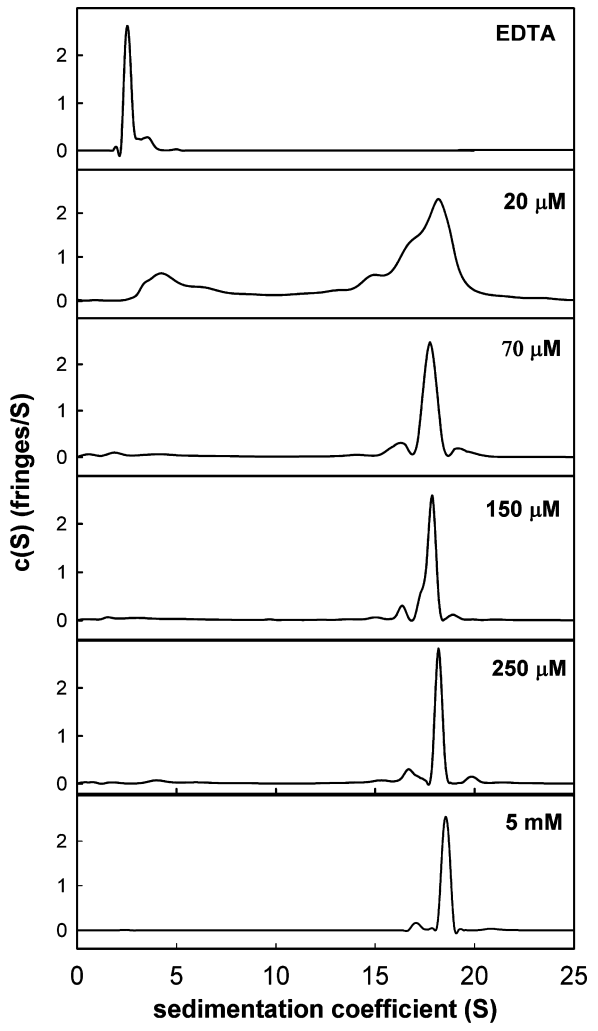

Figure 2. Sedimentation velocity analysis of FtsZ in the presence of 1 mM GMPCPP at variable Mg^{2+} concentration: Sedimentation profiles of 0.5 g/L FtsZ equilibrated in working buffer at the magnesium concentrations specified in the figure.

dx.doi.org/10.1021/bi300401b | Biochemistry 2012, 51, 4541−4550

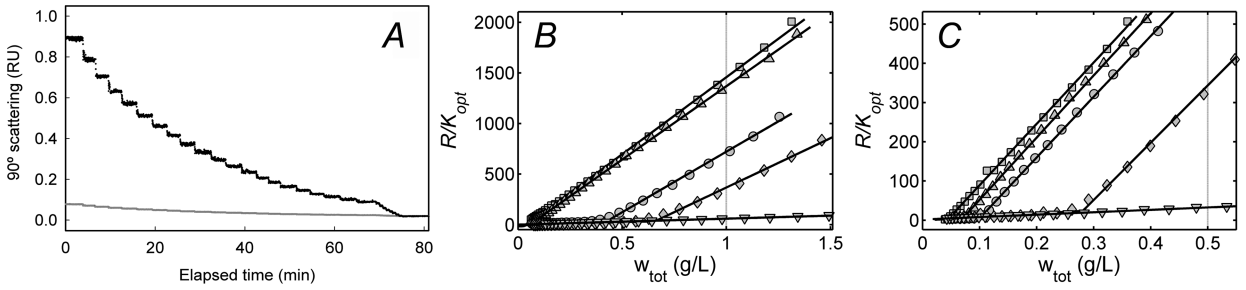

Figure 3. Mg^{2+} dependence of FtsZ composition gradient light scattering (90°, 690 nm). (A) Light scattering of a FtsZ solution (initial concentration around 1 g/L) in working buffer in the presence of 1 mM GTP with 5 mM Mg^{2+} (black) or EDTA (gray), both supplemented with RS, plotted as a function of the elapsed time through a dilution experiment. (B, C) Concentration dependence of GTP-FtsZ and GMPCPP-FtsZ static light scattering at 90°, respectively. From top to bottom, Mg^{2+} content was 5 mM, 300 μM, 100 μM, and 20 μM (B) and 5 mM, 100 μM, 50 μM, and 20 μM (C). Scattering profiles showing only a small dependence of scattering upon concentration were obtained from solutions containing 2 mM EDTA. Curves represent best-fits of the solubility model to each data set, calculated using eq 6 with best-fit parameter values given in Table 1. Vertical dashed lines depict the FtsZ concentrations at which sedimentation velocity experiments in Figures 1 and 2 were conducted.

the distribution of sedimentation coefficients is quantitatively described by a single sharp sedimenting boundary with an average *s*-value of 18−19 S, significantly higher than that characterizing the sedimentation of FtsZ polymers in the presence of GTP. This difference in *s*-value could in principle be attributed to differences in average mass and/or conformation, but additional data to be described below will indicate that the difference may be attributed exclusively to differences in average mass. The $c(s)$ distributions at intermediate Mg^{2+} showed that below 70 μM Mg^{2+} polymers induced by GMPCPP sedimented primarily as a mixture of rapidly sedimenting (18−19 S) and slowly sedimenting (~3 S) species, with only a minor contribution from intermediate species. The most remarkable difference with GTP-FtsZ polymers regarding the effect of magnesium is that, in the presence of GMPCPP, the observed sedimentation coefficient of rapidly sedimenting protein remained invariant through the whole Mg^{2+} concentration range assayed (i.e., at 20 μM and above). In the presence of EDTA, FtsZ sedimented as a main single species with an *s*-value around 2.5 S, similar to the value obtained under the same conditions but in the presence of GTP instead of GMPCPP (see above). Hence the presence of EDTA, under our conditions, precluded the formation of polymers irrespective of the nucleotide triggering polymerization.

Concentration-Dependent 90° Static Light Scattering. In Figure 3A the relative intensity of 690-nm light scattered at 90° recorded in a typical experiment is plotted as a function of time for a set of serial dilutions for FtsZ equilibrated in working buffer with 5 mM Mg^{2+} (black) or EDTA (gray) in the presence of 1 mM GTP supplemented with GTP-RS. The calculated concentration dependence of scattering intensity, expressed as the scaled Rayleigh ratio (see Experimental Procedures) measured at different Mg^{2+} concentrations over a broad range of FtsZ concentrations (0.1−1.5 g/L), is plotted in Figure 3B. The results of corresponding measurements of the dependence of the 90° static light scattering of FtsZ upon the concentration of protein in the presence of GMPCPP and various concentrations of Mg^{2+} are plotted in Figure 3C. The outstanding qualitative feature of the measured dependence of scattering intensity upon concentration at fixed Mg^{2+} in both nucleotides is a concerted transition between a region at low concentration with a low slope and a second region at higher concentration with a substantially greater slope. These data may be used to test the hypothesis that below a certain "critical concentration" comparable to a solubility, w_{sol}, the protein exists primarily as a single species or narrow distribution of low molecular weight scatterers, $M_{w,low}$, and that all protein in excess of the critical concentration exists as a single species or narrow distribution of high molecular weight scatterers, the mean size of which is approximately independent of the amount of scatterer. As we assume that for a given concentration of Mg^{2+} the size of the large scatterers is (approximately) independent of total concentration, we can define an apparent molar mass, $M_{w,high}^{apparent}$, equal to the product of the true molar mass times a constant attenuation factor equal to the ratio of the intensity of scattering at 90° to that at 0°, which will be subsequently shown to be on the order of one-third. We then propose that the concentration dependence may be approximately described by the following two-state model:

$$\frac{R(w, 90^\circ)}{K_{opt}} = w_{low}M_{w,low} + w_{high}M_{w,high}^{apparent} \quad (6)$$

where the proportion of low and high molecular weight scatterers is governed by a quasi-first order phase transition. Thus, for $w_{tot} \leq w_{sol}$, $w_{low} = w_{tot}$, and $w_{high} = 0$, and for $w_{tot} > w_{sol}$, $w_{low} = w_{sol}$, and $w_{high} = w_{tot} - w_{sol}$. Equation 6 was fit to the combined data for each nucleotide at each Mg^{2+} concentration. The best fit of this equation to each data set is plotted together with the data in Figure 3B,C, and the best-fit parameter values are presented in Table 1.

Concentration-Dependent Multiangle Light Scattering. The normalized scattering intensity of a solution of FtsZ in 1 mM GTP + RS + 5 mM Mg^{2+} is plotted as a function of concentration and $\sin^2(\theta/2)$ in Figure 4A, and data obtained from a solution of FtsZ in 0.4 mM GMPCPP + 5 mM Mg^{2+} are plotted in Figure 4B. In both cases the angular dependence of scattering is evident. These data were analyzed in the context of the solubility model described above, modified to allow empirically for the dependence of the scattering of high molecular weight species upon θ:

$$\frac{R(w_{tot}, \theta)}{K_{opt}} = w_{low}M_{w,low} + w_{high}M_{w,high}(1 + A_1 g + A_2 g^2) \quad (7)$$

where $g = \sin^2(\theta/2)$. A surface calculated according to the best least-squares fit of eq 7 to the combined data, using the best-fit parameter values given in the figure caption, is plotted together with the data in Figure 4A,B. The goodness of fit may be seen

dx.doi.org/10.1021/bi300401b | *Biochemistry* 2012, 51, 4541−4550

Table 1. Values of Best-Fit Parameters Obtained by Fitting eq 6 to the 90° Scattering Data Plotted in Figure 3B,C[a]

nucleotide	$[Mg^{2+}]$	w_{sol} (g/L)	$M_{w,high}^{apparent}$
GTP	0 (EDTA)		
	20 μM	0.66	9.8×10^5
	100 μM	0.42	1.2×10^6
	300 μM	0.058	1.45×10^6
	5 mM	0.044	1.52×10^6
GMPCPP	0 (EDTA)		
	20 μM	0.28	1.46×10^6
	50 μM	0.10	1.55×10^6
	100 μM	0.07	1.59×10^6
	5 mM	0.045	1.56×10^6

[a]Values of $M_{w,low}$ were determined by analysis of the data in the presence of EDTA, 60 000 for GTP and 61 500 for GMPCPP, and subsequently used as constrained parameter for the fits in the presence of the different magnesium concentrations.

more clearly in the anaglyphic figures and movies provided in Supporting Information.

The results of fitting the solubility model to the data obtained in the presence of both GTP and GMPCPP indicate that the "solubility" of low molecular weight scatterer is too low to be distinguishable from zero with current experimental precision. Data obtained from the GMPCPP + 5 mM Mg^{2+} solutions are compatible with a value of $M_{w,high}$ between 5.7 and 7.0×10^6, corresponding to a mean oligomer stoichiometry between 145 and 175 monomers. Data obtained from the GTP + RS + 5 mM Mg^{2+} are compatible with a value of $M_{w,high}$ between 4.2 and 4.8×10^6, corresponding to a mean oligomer stoichiometry between 105 and 120 monomers.

Fluorescence Correlation Spectroscopy. Fluorescence autocorrelation functions obtained at constant protein concentration and various Mg^{2+} concentrations in the presence of GTP + RS are plotted in Figure 5A. Comparable data obtained in the presence of GMPCPP are plotted in Figure 5B. In both panels the shift toward longer relaxation times with increasing Mg is evident and may be attributed to the increasing abundance of larger species with smaller diffusion coefficients. The data were fitted to within experimental precision by eq 4 with three fluorescent species: a rapidly diffusing free dye, a more slowly diffusing labeled monomeric FtsZ, and a very slowly diffusing labeled polymeric FtsZ. In the presence of GTP + RS, the autocorrelation function becomes essentially independent of Mg^{2+} concentration at concentrations exceeding ~0.4 mM (Figure 5A), and in the presence of GMPCPP, the autocorrelation function becomes essentially independent of Mg^{2+} concentration at concentrations exceeding ~0.1 mM (Figure 5B). These results accord semiquantitatively with the Mg^{2+} dependence of polymer formation monitored by sedimentation velocity (Figures 1 and 2) and 90° light scattering (Figure 3B,C). The best fit value of the diffusion coefficient of polymer at 5 mM Mg^{2+} was $4.1 \pm 0.3 \times 10^{-8}$ cm^2/s in GTP + RS and $3.1 \pm 0.4 \times 10^{-8}$ cm^2/s in GMPCPP (Figure 5E).

Fluorescence autocorrelation functions obtained for different protein concentrations in the presence of 5 mM Mg^{2+} and GTP + RS are plotted in Figure 6A, and comparable data obtained in the presence of GMPCPP are plotted in Figure 6B. In both cases the autocorrelation functions become almost independent of protein concentration at concentrations exceeding ~0.5 g/L, indicating that at these concentrations almost all of the protein exists as high molecular weight species of constant size. The limiting values of the diffusion coefficients of polymer in GTP + RS and in GMPCPP are the same as obtained from analysis of Mg^{2+} dependence as described above (Figure 6E) to within the uncertainties specified above. Interestingly, early detection of polymers in the presence of GTP occurred at concentrations slightly above 0.05 g/L coinciding with the critical concentration of polymerization of FtsZ under these conditions.[6,9,14] In the presence of EDTA and GTP or GMPCPP, the fluorescence autocorrelation curves overlap with those obtained for the unassembled protein.

Dynamic Light Scattering and Estimate of Molar Masses from Hydrodynamic Measurements. Autocorrelation functions obtained at a constant concentration of protein showed a significant shift to longer times with increasing Mg^{2+} concentration both in the presence of GTP + RS and GMPCPP (Figure 5C,D). In accordance with FCS data, GTP-FtsZ polymers showed a significant increase of the translational diffusion coefficient of assembled FtsZ with decreasing Mg^{2+} concentrations (Figure 5C), while GMPCPP-FtsZ polymers existed as a defined species with a translational diffusivity that did not depend on Mg^{2+} concentration above 20−50 μM (Figure 5D), also in good agreement with the sedimentation velocity and static light scattering results (Figures 1−3). The translational mobility of

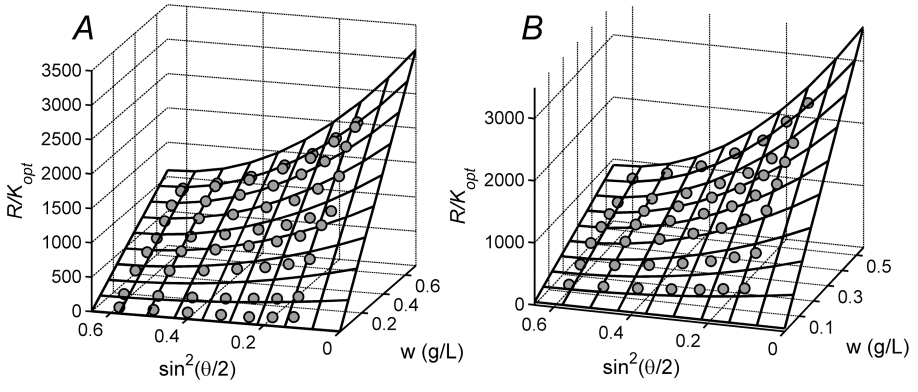

Figure 4. Angular and concentration dependence of scattering of FtsZ polymers in 5 mM Mg^{2+} and GTP + RS (A) or GMPCPP (B). Scattering intensity plotted as a function of the w/v FtsZ concentration and $\sin^2(\theta/2)$. Black mesh surface is the best fit of the solubility model to the experimental data (symbols), calculated using eq 7 with the following best-fit parameter values. For GTP + RS, $w_{sol} = 0$, $M_{w,high} = 4.5\ (\pm 0.3) \times 10^6$, $A_1 = -2.05$, $A_2 = 1.61$. For GMPCPP, $w_{sol} = 0$, $M_{w,high} = 6.4\ (\pm 0.7) \times 10^6$, $A_1 = -2.37$, $A_2 = 1.86$.

dx.doi.org/10.1021/bi300401b | Biochemistry 2012, 51, 4541−4550

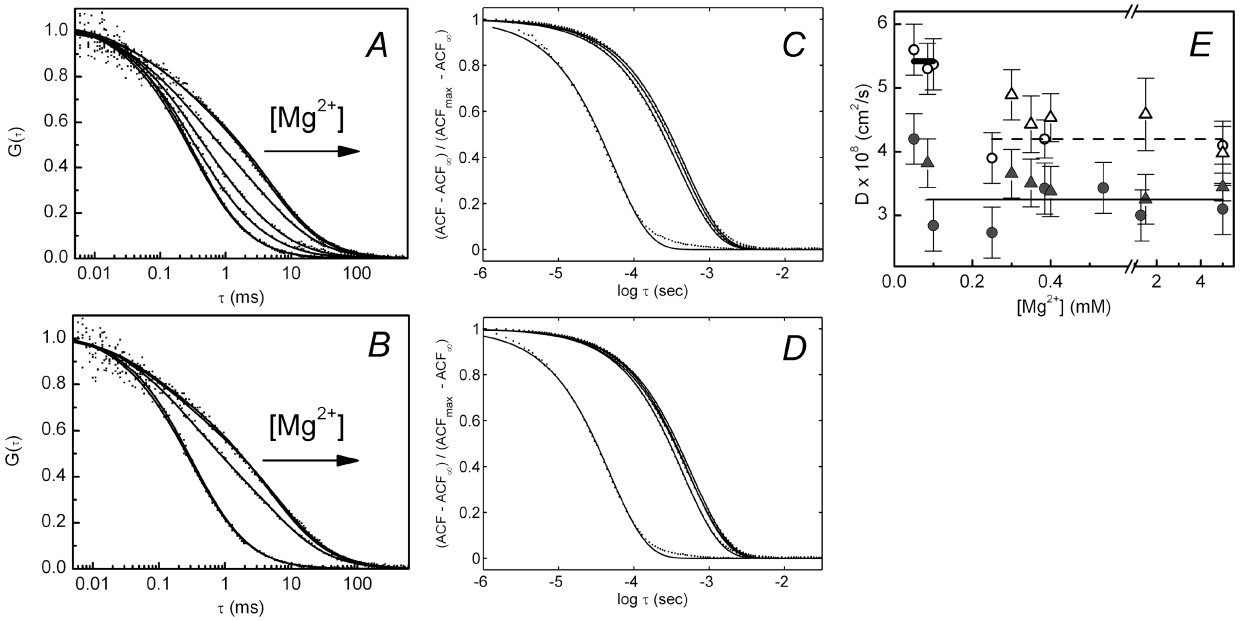

Figure 5. Dependence with $MgCl_2$ concentration of translational diffusion properties of FtsZ polymers formed in GTP + RS or GMPCPP. (A, B) Normalized FCS autocorrelation curves of GTP-FtsZ and GMPCPP-FtsZ polymers, respectively. From faster to slower diffusion, $MgCl_2$ content was 0, 50, 100, 250, 385 μM and 5 mM (A, GTP, the last two indistinguishable) and 0, 50, 250 μM and 5 mM (B, GMPCPP, the last two indistinguishable). Samples without Mg^{2+} contain 1 mM EDTA and overlap with unassembled FtsZ-Alexa488 (no GTP or GMPCPP added). The fractional contribution of unassembled FtsZ to the profiles with GTP was 15−20% (1 mM-385 μM), 32% (250 μM), 53% (100 μM), and 67% (50 μM $MgCl_2$), and with GMPCPP 15−20% (5 mM-250 μM) and 29% (50 μM $MgCl_2$). Solid lines are the fits of the models indicated in the main text. Concentration of FtsZ-Alexa 488 was 0.006 g/L and unlabeled FtsZ was added up to 1 g/L. (C, D) Normalized DLS autocorrelation curves of GTP-FtsZ (1 g/L FtsZ) and GMPCPP-FtsZ (0.5 g/L FtsZ) polymers, respectively. From faster to slower diffusion, $MgCl_2$ content was 0, 300, 350 μM and 5 mM (*C*, GTP, those with Mg^{2+} similar within error) and 0, 200, 300 μM, 1.5 and 5 mM (D, GMPCPP, last three similar within error). Samples without Mg^{2+} contain 1 mM EDTA. Solid lines are the fits of the model indicated in the main text. (E) Dependence of the normalized translational diffusion coefficient of GTP- (open) and GMPCPP-FtsZ polymers (solid) determined by DLS (triangles) and FCS (circles). Data are the average of at least three independent experiments ± SD. Horizontal traces depict the average diffusion values calculated over the concentration independent range, 4.2×10^{-8} (GTP) and 3.2×10^{-8} cm^2/s (GMPCPP).

FtsZ polymers in GMPCPP, according to the *D*-values measured both by FCS and DLS, was systematically slower than that previously measured for FtsZ in GTP under the same conditions (Figure 5E), in agreement with a larger size for the 19 S species that FtsZ forms in the presence of GMPCPP at high Mg^{2+}. The data were fitted to within experimental precision by eq 3 rendering best fit values of the diffusion coefficients of polymer in the high Mg^{2+} concentration limit of $4.0 \pm 0.5 \times 10^{-8}$ cm^2/s in GTP + RS and $3.4 \pm 0.2 \times 10^{-8}$ cm^2/s in GMPCPP (Figure 5E).

DLS autocorrelation functions obtained at different FtsZ concentrations with 5 mM Mg^{2+} and GTP + RS or GMPCPP are plotted in Figure 6, panels C and D, respectively. As observed by FCS, profiles become almost independent of protein concentration above ∼0.5 g/L FtsZ, verifying our previous findings that the concentration dependence of the $c(s)$ distribution of GTP-FtsZ was compatible with the concerted formation of a narrow distribution of favored oligomers (13 S) whose apparent size does not increase between 0.4 and 1.5 g/L FtsZ.[9]

The apparent molar masses calculated from the diffusion values, average of FCS and DLS, and sedimentation coefficients according to eq 5 are 3.4×10^6 g (∼85 FtsZ molecules/oligomer) for the GTP-FtsZ polymer and 6.0×10^6 g (∼150 FtsZ molecules/oligomer) for the GMPCPP-FtsZ polymer. Although the diffusion coefficients from DLS data account for the diffusing properties of all species in solution, it should be noted that the measured autocorrelation function will be mainly contributed by the bigger species. Therefore, under conditions at which polymers are formed, translational diffusion coefficients obtained by DLS should be directly comparable to those obtained by FCS for the slowly diffusing polymeric FtsZ, since the contribution of unassembled species (given their low concentration and much smaller size) is negligible. This might be also the case for the smaller GTP-FtsZ oligomer formed at micromolar Mg^{2+} (∼40 FtsZ subunits as calculated from *D* and *s* via the Svedberg equation).

■ DISCUSSION

Comparison of the results obtained by measurement of sedimentation velocity and 90° light scattering provides a consistent and unequivocal picture of the mechanism of FtsZ self-assembly in the presence of GTP. The results shown in Figure 1 (GTP + RS) were obtained from solutions containing 1 g/L protein, indicated by a dashed vertical line in Figure 3B. In the presence of EDTA the scattering signal is consistent with an average molecular weight corresponding to a mixture of monomeric and dimeric FtsZ, in qualitative agreement with sedimentation velocity results. In the presence of 100 μM Mg^{2+}, the scattering data indicate a mixture of approximately 40% low molecular weight species and 60% high molecular weight species, again in good agreement with the distribution of sedimentation coefficients shown in Figure 1. In the presence of 5 mM Mg^{2+} almost complete (>95%) conversion of protein to an even higher molecular weight species occurs, once again in qualitative agreement with the distribution of sedimentation

dx.doi.org/10.1021/bi300401b | *Biochemistry* 2012, 51, 4541−4550

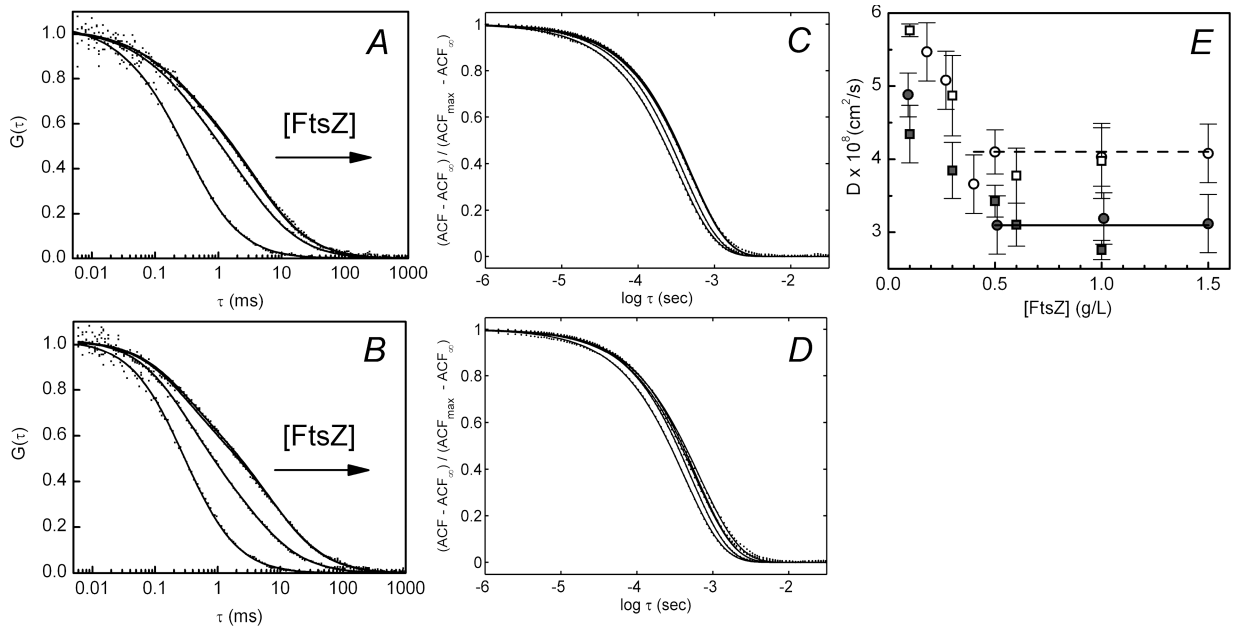

Figure 6. Concentration dependence of translational diffusion of GTP and GMPCPP FtsZ polymers. (A, B) Normalized FCS autocorrelation curves of FtsZ polymers formed in the presence of 1 mM GTP or 0.4−1 mM GMPCPP, respectively. From faster to slower diffusion, 0.006, 0.27, 0.5, and 1.5 g/L FtsZ (A, GTP, last two overlap) and 0.006, 0.09, 0.5, and 1 g/L FtsZ (B, GMPCPP, last two superimposable). The fractional contribution of unassembled FtsZ to the autocorrelation profiles with GTP was ∼10% (1.5−0.5 g/L) and 24% (0.27 g/L), and with GMPCPP ∼10% (1−0.5 g/L) and 40% (0.09 g/L). Concentration of FtsZ-Alexa 488 was 0.006 g/L and additional unlabeled FtsZ was added up to the final concentration specified. (C, D) Normalized DLS autocorrelation curves of FtsZ polymers formed in the presence of 1 mM GTP or 0.4 mM GMPCPP, respectively. From faster to slower diffusion: 0.1, 0.3, 0.5, 0.6, and 1.0 g/L FtsZ. Profiles at 0.5−1.0 g/L overlap for GTP and are similar, within error, for GMPCPP. (E) Dependence with FtsZ concentration of the normalized apparent diffusion coefficient of GTP- (open) and GMPCPP-FtsZ polymers (solid) determined by DLS (squares) and FCS (circles). Horizontal lines indicate the average diffusion value of the concentration independent polymeric species, 4.2×10^{-8} (GTP) and 3.2×10^{-8} cm^2/s (GMPCPP).

coefficients shown in Figure 1. Taken together, the scattering data indicate that the mean size of the high molecular weight species is approximately independent of protein concentration, but gradually increases with increasing Mg^{2+} concentration, apparently attaining a maximum size between 350 μM and 1 mM, again in qualitative agreement with the results shown in Figure 1.

The results shown in Figure 2 (GMPCPP) were obtained from solutions containing 0.5 g/L protein, indicated by a dashed vertical line in Figure 3C. In the absence of added Mg^{2+}, the scattering profile is consistent with an average molecular weight between that of monomeric and dimeric FtsZ, consistent with the results shown in Figure 2. In the presence of 20 μM Mg^{2+}, the scattering profile is consistent with the presence of comparable amounts of both low and high molecular weight species, in qualitative accord with the distribution of sedimentation coefficients obtained from sedimentation velocity experiments. At higher Mg^{2+} concentrations, the scattering profile suggests the presence of predominantly high molecular weight scatterers, the mean size of which is insensitive to changes in Mg^{2+} concentration. This last result, which differs from that found in the presence of RS, is once again in qualitative accord with distribution of sedimentation coefficients obtained from the sedimentation velocity experiments.

Taken together, the sedimentation velocity data and 90° scattering data provide strong evidence for a highly concerted transition, thermodynamically similar to a second-order phase transition, between a paucidisperse size distribution of low molecular weight oligomers, and a paucidisperse size distribution of high molecular weight oligomers. Both of these observations, together with the results of angle-dependent static light scattering, dynamic light scattering, and fluorescence correlation spectroscopy, rule out mechanisms based solely upon incremental growth of oligomer via sequential addition of monomers, and any scheme leading to unbounded polymer size. The control experiments conducted in the presence of the slowly hydrolyzable analogue of GTP exhibit identical qualitative behavior, indicating that the observed growth scheme is not attributable in essence to a nonequilibrium steady-state reaction cycle involving GTP hydrolysis and GTP-GDP exchange, although these factors are likely to modulate the observed behavior, as discussed below.

The mean size of polymer in 5 mM Mg^{2+} was estimated to be 115 ± 8 in GTP + RS and 160 ± 15 in GMPCPP on the basis of a two-state analysis of angle- and concentration-dependent light scattering. The mean size of polymer was also independently estimated from approximate analyses of the results of measurements of the sedimentation and diffusion coefficients by means of eq 5. The values obtained from this relation for the stoichiometry of polymers in GTP and GMPCPP are 85 ± 7 and 150 ± 10 respectively. The quantitative (but not qualitative) difference between the values obtained by the two different approaches may be attributed at least in part to the fact that both analyses depend upon two-state approximations applied in rather different contexts.

Molecular weight distributions estimated using the SEDFIT $c(M)$ analysis are presented in Supporting Information. These distributions are consistent with estimates of the average molar mass of oligomers and the uncertainty of these estimates derived from hydrodynamic and light scattering data as described in the text.

dx.doi.org/10.1021/bi300401b | *Biochemistry* 2012, 51, 4541−4550

Although the self-assembly of FtsZ in GTP qualitatively resembles that in GMPCPP, significant quantitative differences are present. (a) The average size of polymer varies with Mg^{2+} concentration in GTP, whereas it does not in GMPCPP. (b) The cooperative transition between low and high molecular weight distributions appears to be sharper and more similar to a first-order phase transition in the presence of GMPCPP than in GTP. (c) The average size of polymer in the presence of high Mg^{2+} is significantly larger in GMPCPP than in GTP. It is clear that nonequilibrium steady-state effects arising from GTP hydrolysis and GTP-GDP exchange cannot be responsible for the concerted nature of the transition between low and high molecular weight species observed in the presence of both GTP + RS and GMPCPP, since the cooperativity of the transition is more pronounced in the presence of the much more slowly hydrolyzable GTP analogue.

Fragmentation certainly can limit the size of fibrillar oligomers, but by itself cannot elicit a highly concerted formation of a narrow distribution of favored polymers in a manner resembling a phase transition, as we observe here. The results clearly indicate that there is no significant amount of material existing as oligomers intermediate between a low molecular weight distribution consisting mainly of monomers and dimers, and a narrow high molecular weight oligomeric species of stoichiometry between 80 and 180 (depending upon the nucleotide used to promote FtsZ assembly). The major consequence of fragmentation and annealing of fibrils would be to accelerate the approach to equilibrium. The rapid exchange of FtsZ subunits when mixing donor-labeled and acceptor-labeled FtsZ fibrils in the FRET experiments done by Erickson and co-workers[11] does not require the disappearance of fibrils, merely transient breakage and closure along the length of a fibril. The essential point is that without a mechanism for formation of a discrete oligomer or narrow molecular weight distribution of fibrillar oligomers in a highly cooperative fashion, nucleation + fragmentation alone will not account for the data.

In summary, the combined results reported above support the following two major conclusions:

(1) The self-assembly of FtsZ under the conditions of this study proceeds by a concerted transition, thermodynamically resembling a second-order phase transition, between a paucidisperse distribution of low molecular weight species, consisting primarily of monomer and dimer, and a paucidisperse distribution of high molecular weight species (polymer), the size of which is independent of total protein concentration and, in the presence of GMPCPP, is independent of magnesium concentration. It should be kept in mind that this mode of self-assembly may not necessarily apply under other experimental conditions, as it is well-known that the structure of noncovalent oligomers/polymers formed by proteins in general, and FtsZ in particular, may vary considerably depending upon solution conditions (see, for example, ref 2 and references therein).

(2) In the limit of high magnesium concentration, the average size of polymer is estimated to lie between 80 and 120 FtsZ protomers in the presence of GTP + RS, and between 140 and 180 FtsZ protomers in the presence of GMPCPP.

The purpose of the present report is not to advocate any particular molecular model for fibril formation, but to present a substantial body of experimental data obtained via several biophysical methods that is self-consistent and, in our opinion, must be taken into account in any future attempt to formulate a mechanistic scheme for FtsZ self-assembly.

We do not claim physiological significance to the presence and narrow size distribution of high molecular weight oligomers, indicated by our data, since the system studied here is highly simplified and lacks the companion proteins and surfaces required to assemble the septal ring in vivo. The work presented here and in other studies (reviewed in refs 2 and 4) clearly indicates that FtsZ may self-assemble polymorphically, and the product or products of self-assembly may vary qualitatively with the conditions under which self-assembly is studied. Thus the results presented here neither confirm nor refute a contrasting model, based upon data obtained under rather different conditions, according to which the physiological Z-ring situated at and encircling the midpoint of the cell prior to the onset of cell division consists of a series of short overlapping protofilaments of FtsZ.[2,27,28] However, the characterization of FtsZ solution behavior under the conditions of this study provides information that we believe will ultimately be integrated into more complex schemes describing systems containing the additional elements referred to above.

■ ASSOCIATED CONTENT

Supporting Information

Anaglyphic figures showing the normalized scattering intensity of a solution of FtsZ in 1 mM GTP + RS + 5 mM Mg^{2+} (Supplementary Figure S1) and FtsZ in 0.4 mM GMPCPP + 5 mM Mg^{2+} (Supplementary Figure S2) as a function of concentration and $\sin^2(\theta/2)$. Figure S3 shows the molar mass $c(M)$ distributions calculated using SEDFIT from the $c(s)$ distributions and the externally determined frictional ratio for the GTP and GMPCPP forms of FtsZ at mM Mg^{2+}. Movies showing the normalized scattering intensity of a solution of FtsZ in 1 mM GTP + RS + 5 mM Mg^{2+} (Supplementary Movie 1) and FtsZ in 0.4 mM GMPCPP + 5 mM Mg^{2+} (Supplementary Movie 2) are plotted as a function of concentration and $\sin^2(\theta/2)$ rotating about the z-axis. This material is available free of charge via the Internet at http://pubs.acs.org.

■ AUTHOR INFORMATION

Corresponding Author

*E-mail: grivas@cib.csic.es. Phone: +34 918373112.

Funding

This work was supported by the Spanish Ministerio de Ciencia e Innovación through Grants BIO2008-04478-C03 and BIO2011-28941-C03-03 to G.R. and BFU2010-14910 and BIO2011-28941-C03-02 to S.Z.; by the European Commission through contract HEALTH-F3-2009-223432, by Human Frontiers Science Program through Grant RGP0050/2010-C102, and Comunidad de Madrid through Grant S-BIO-0260/2006 to G.R.; and by the CSIC through Grants 200980I186 and 201020I001 to S.Z. and C.A., respectively. B.M. is a JAE postdoctoral associate from the European Social Fund and the Spanish Consejo Superior de Investigaciones Científicas (CSIC). R.A.G. is a predoctoral fellow from the CSIC-JAE program. Research of APM is supported by the Intramural Research Program of the National Institute of Diabetes and Digestive and Kidney Diseases, National Institutes of Health, U.S. Department of Health and Human Services.

Notes

The authors declare no competing financial interest.

■ ACKNOWLEDGMENTS

We especially thank J. Mingorance for critically reading the manuscript and for his helpful suggestions. We also thank C.A. Royer for the loan of a two-photon laser and for her advice; A. Ortega, J. García de la Torre, and A. U. Acuña for helpful discussions; an anonymous reviewer for valuable comments; and C. Fernández for advice in the instrumental setup for 90° scattering measurements.

■ ABBREVIATIONS USED

RS, GTP regeneration system; GMPCPP, guanosine-5-[(α,β)-methyleno]triphosphate, sodium salt; GTP-FtsZ and GMPCPP-FtsZ polymers, polymers of FtsZ where assembly was triggered by GTP or GMPCPP, respectively

■ REFERENCES

(1) Adams, D. W., and Errington, J. (2009) Bacterial cell division: assembly, maintenance and disassembly of the Z ring. *Nat. Rev. Microbiol. 7*, 642−653.

(2) Erickson, H. P., Anderson, D. E., and Osawa, M. (2010) FtsZ in bacterial cytokinesis: cytoskeleton and force generator all in one. *Microbiol. Mol. Biol. Rev. 74*, 504−528.

(3) Margolin, W. (2000) Organelle division: Self-assembling GTPase caught in the middle. *Curr. Biol. 10*, R328−330.

(4) Mingorance, J., Rivas, G., Vélez, M., Gómez-Puertas, P., and Vicente, M. (2010) Strong FtsZ is with the force: mechanisms to constrict bacteria. *Trends Microbiol. 18*, 348−356.

(5) Rivas, G., López, A., Mingorance, J., Ferrándiz, M. J., Zorrilla, S., Minton, A. P., Vicente, M., and Andreu, J. M. (2000) Magnesium-induced linear self-association of the FtsZ bacterial cell division protein monomer. The primary steps for FtsZ assembly. *J. Biol. Chem. 275*, 11740−11749.

(6) González, J. M., Jiménez, M., Vélez, M., Mingorance, J., Andreu, J. M., Vicente, M., and Rivas, G. (2003) Essential cell division protein FtsZ assembles into one monomer-thick ribbons under conditions resembling the crowded intracellular environment. *J. Biol. Chem. 278*, 37664−37671.

(7) Mingorance, J., Tadros, M., Vicente, M., González, J. M., Rivas, G., and Vélez, M. (2005) Visualization of single *Escherichia coli* FtsZ filament dynamics with atomic force microscopy. *J. Biol. Chem. 280*, 20909−20914.

(8) Popp, D., Iwasa, M., Narita, A., Erickson, H. P., and Maeda, Y. (2009) FtsZ condensates: an in vitro electron microscopy study. *Biopolymers 91*, 340−350.

(9) González, J. M., Vélez, M., Jiménez, M., Alfonso, C., Schuck, P., Mingorance, J., Vicente, M., Minton, A. P., and Rivas, G. (2005) Cooperative behavior of Escherichia coli cell-division protein FtsZ assembly involves the preferential cyclization of long single-stranded fibrils. *Proc. Natl. Acad. Sci. U. S. A. 102*, 1895−1900.

(10) Stricker, J., Maddox, P., Salmon, E. D., and Erickson, H. P. (2002) Rapid assembly dynamics of the *Escherichia coli* FtsZ-ring demonstrated by fluorescence recovery after photobleaching. *Proc. Natl. Acad. Sci. U. S. A. 99*, 3171−3175.

(11) Chen, Y., and Erickson, H. P. (2005) Rapid in vitro assembly dynamics and subunit turnover of FtsZ demonstrated by fluorescence resonance energy transfer. *J. Biol. Chem. 280*, 22549−22554.

(12) Salvarelli, E., Krupka, M., Rivas, G., Vicente, M., and Mingorance, J. (2011) Independence between GTPase active sites in the Escherichia coli cell division protein FtsZ. *FEBS Lett. 585*, 3880−3883.

(13) Jiménez, M., Martos, A., Vicente, M., and Rivas, G. (2011) Reconstitution and organization of *Escherichia coli* proto-ring elements (FtsZ and FtsA) inside giant unilamellar vesicles obtained from bacterial inner membranes. *J. Biol. Chem. 286*, 11236−11241.

(14) Reija, B., Monterroso, B., Jimenez, M., Vicente, M., Rivas, G., and Zorrilla, S. (2011) Development of a homogeneous fluorescence anisotropy assay to monitor and measure FtsZ assembly in solution. *Anal. Biochem. 418*, 89−96.

(15) Schuck, P. (2000) Size-distribution analysis of macromolecules by sedimentation velocity ultracentrifugation and lamm equation modeling. *Biophys. J. 78*, 1606−1619.

(16) Attri, A. K., and Minton, A. P. (2005) Composition gradient static light scattering: a new technique for rapid detection and quantitative characterization of reversible macromolecular hetero-associations in solution. *Anal. Biochem. 346*, 132−138.

(17) Kameyama, K., and Minton, A. P. (2006) Rapid quantitative characterization of protein interactions by composition gradient static light scattering. *Biophys. J. 90*, 2164−2169.

(18) Fernández, C., and Minton, A. P. (2008) Automated measurement of the static light scattering of macromolecular solutions over a broad range of concentrations. *Anal. Biochem. 381*, 254−257.

(19) Schmitz, K. S. (1990) *An Introduction to Dynamic Light Scattering by Macromolecules*, Chapter 2, Academic Press, Boston.

(20) Kita, R., Takahashi, A., Kaibara, M., and Kubota, K. (2002) Formation of fibrin gel in fibrinogen-thrombin system: static and dynamic light scattering study. *Biomacromolecules 3*, 1013−1020.

(21) Skakun, V. V., Hink, M. A., Digris, A. V., Engel, R., Novikov, E. G., Apanasovich, V. V., and Visser, A. J. (2005) Global analysis of fluorescence fluctuation data. *Eur. Biophys. J. 34*, 323−334.

(22) Bacia, K., and Schwille, P. (2007) Practical guidelines for dual-color fluorescence cross-correlation spectroscopy. *Nat. Protoc. 2*, 2842−2856.

(23) Culbertson, C. T., Jacobson, S. C., and Michael Ramsey, J. (2002) Diffusion coefficient measurements in microfluidic devices. *Talanta 56*, 365−373.

(24) Gendron, P. O., Avaltroni, F., and Wilkinson, K. J. (2008) Diffusion coefficients of several rhodamine derivatives as determined by pulsed field gradient-nuclear magnetic resonance and fluorescence correlation spectroscopy. *J. Fluoresc. 18*, 1093−1101.

(25) Svedberg, T., Pedersen, K. O. (1940) *The Ultracentrifuge*, Oxford, Clarendon Press.

(26) Reisler, E., Cheung, P., and Borochov, N. (1986) Macro-molecular assemblies of myosin. *Biophys. J. 49*, 335−342.

(27) Fu, G., Huang, T., Buss, J., Coltharp, C., Hensel, Z., and Xiao, J. (2010) In vivo structure of the E. coli FtsZ-ring revealed by photoactivated localization microscopy (PALM). *PLoS One 5*, e12682.

(28) Li, Z., Trimble, M. J., Brun, Y. V., and Jensen, G. J. (2007) The structure of FtsZ filaments in vivo suggests a force-generating role in cell division. *EMBO J. 26*, 4694−4708.